CHAPTER V

RESULTS AND DISCUSSIONS

To understand the limitations of our automated algorithm in analyzing plasma parameters, I-V characteristic data obtained from each discharge shall be analyzed. In each discharge, the comparative results between the manual calculation and the automated algorithm will be presented. Then, limitations of the automated algorithm to yield accurate results will be discussed.

5.1 Analytical Results of DC Discharge

An example of I-V characteristic of probe measurement in a DC discharge is shown in figure 5.1. The data were acquired in air plasma by varying the current flow between two electrodes and changing pressures from 0.6 to 1 torr. The acquisition was done by a single probe located at 5 centimeter from the cathode plate.

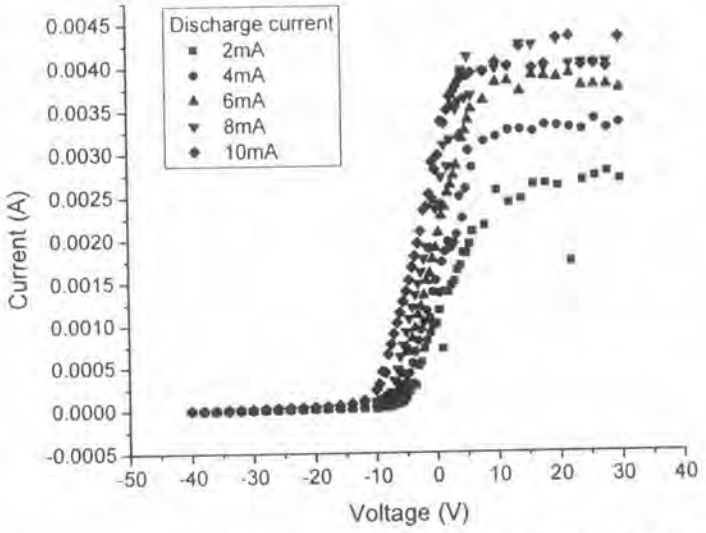

Figure 5.1: Example of the I-V characteristic of a DC discharge at the pressure of 1 torr and various discharge currents.

The analytical results of both the manual calculation and the automated algorithm are shown in table 5.1 and 5.2, respectively. Mean and standard derivative results of four parameters i.e. floating and plasma potentials, electron temperature, electron density, obtained from repeating I-V measurements are shown in these tables. However, the ion density is not calculated because of the requirement of the ion mass in calculating this density, the mass of air plasma composes of different gases, including humidity. Therefore, it is not appropriate to put in the mass value of one particle gas into equation (2.18) for ion density.

Table 5.1: Mean and standard derivative (SD) results of plasma parameters obtained from the manual calculation.

Pressure (torr)	current discharge (mA)	manual calculation							
		V_f (V)		V_p (V)		T_e (eV)		N_e (x 10^{10} cm^{-3})	
		mean	SD	mean	SD	mean	SD	mean	SD
0.6	10	-30.00	± 1.15	5.62	± 0.04	2.31	± 0.21	1.31	± 0.05
	8	-28.67		6.83		2.09		1.30	
	6	-28.00		7.57		2.06		1.19	
	4	-28.00		7.86		2.15		1.00	
	2	-28.00		6.32		1.95		0.61	
0.8	10	-34.00	± 0.00	4.39	± 0.15	2.12	± 0.04	7.02	± 0.06
	8	-32.00		5.27		2.08		6.59	
	6	-32.00		6.18		2.03		5.97	
	4	-32.00		6.76		2.05		5.07	
	2	-32.00		6.18		2.07		3.38	
1	10	-40.00	± 1.15	4.13	± 1.24	2.24	± 0.18	6.72	± 0.32
	8	-36.00		5.31		2.26		6.72	
	6	-36.00		6.52		2.30		6.33	
	4	-36.67		7.79		2.33		5.54	
	2	-37.33		9.25		2.09		3.98	

Table 5.2: Mean and standard derivative (SD) results of plasma parameters obtained from the automated algorithm.

Pressure (torr)	current discharge (mA)	automated algorithm							
		V_f (V)		V_p (V)		T_e (eV)		N_e (x 10^{10} cm^{-3})	
		mean	SD	mean	SD	mean	SD	mean	SD
	10	-30.00		5.97		2.07		1.38	
	8	-28.67		6.39		2.07		1.30	
	6	-28.00	± 1.15	7.03	± 0.04	2.03	± 0.03	1.20	± 0.01
	4	-28.00		6.76		1.94		1.05	
0.6	2	-28.67		6.08		1.93		0.60	
	10	-34.00		2.25		2.01		6.76	
	8	-32.00		2.88		1.94		6.33	
	6	-32.00	± 0.00	3.89	± 0.38	1.77	± 0.08	5.55	± 0.10
	4	-32.00		4.80		1.74		4.63	
0.8	2	-32.00		4.90		1.76		3.12	
	10	-40.00		4.18		2.65		7.15	
	8	-36.00		5.35		2.33		6.82	
	6	-36.00	± 1.15	6.57	± 1.15	2.11	± 0.36	6.09	± 0.64
	4	-36.67		7.79		2.31		5.52	
1	2	-37.33		9.39		2.15		4.01	

From table 5.1 and 5.2 at pressure 0.8 torr, there is a difference of plasma potentials between the manual calculation and the automated algorithm. This difference results from the discrete current in the I-V characteristic of probing measurement, as shown in figure 5.2. The figure shows an example of I-V data at pressure 0.8 torr in the process of defining the transition interval between the automated algorithm (figure 5.2(a)) and the manual calculation (figure 5.2(b)). According to the process of determine plasma potential, the automated algorithm defines the transition interval more narrow than the manual calculation. This is because of the discrete current in the transition region causing the interval of the maximum and minimum of the second derivative to be narrow. Therefore, the slope of the linear fitting of the automated algorithm is steeper than the slope of the manual calculation. This effect lessens plasma potential of the automated algorithm in comparison with the manual calculation.

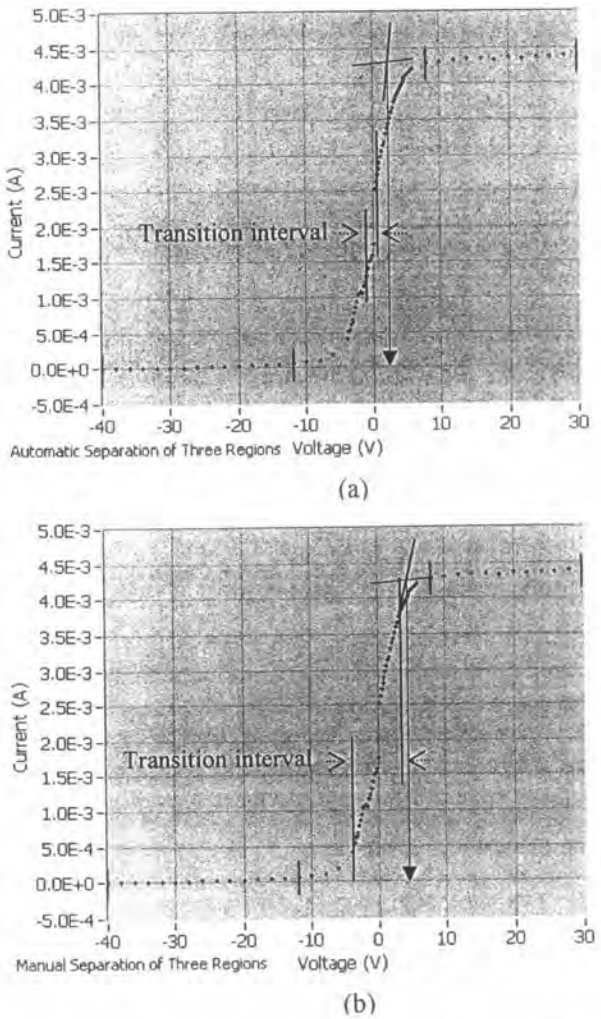

Figure 5.2: An example of the I-V data in the DC discharge probing measurement at pressure 0.8 torr in the process of defining the transition interval between (a) the automated algorithm and (b) the manual calculation.

Figure 5.3 shows the comparative results of plasma parameters at pressure 0.6 torr between the manual calculation and the automated algorithm. From figure 5.3(a), the automated algorithm yields floating potential close to the manual calculation. But, for plasma potential in figure 5.3(b), plasma potentials of the automated algorithm are different from those of the manual calculation in some discharge currents. This is because of discrete current in the transition region, as discussed above. For electron temperature in figure 5.3(c), there is a difference of results between the manual calculation and the automated algorithm in some conditions. This difference arises from the process of defining the ion-saturation region and electron temperature

calculation which shall be discussed in section 5.3. In figure 5.3(d), electron densities obtained from the automated algorithm well agree with the densities of the manual calculation.

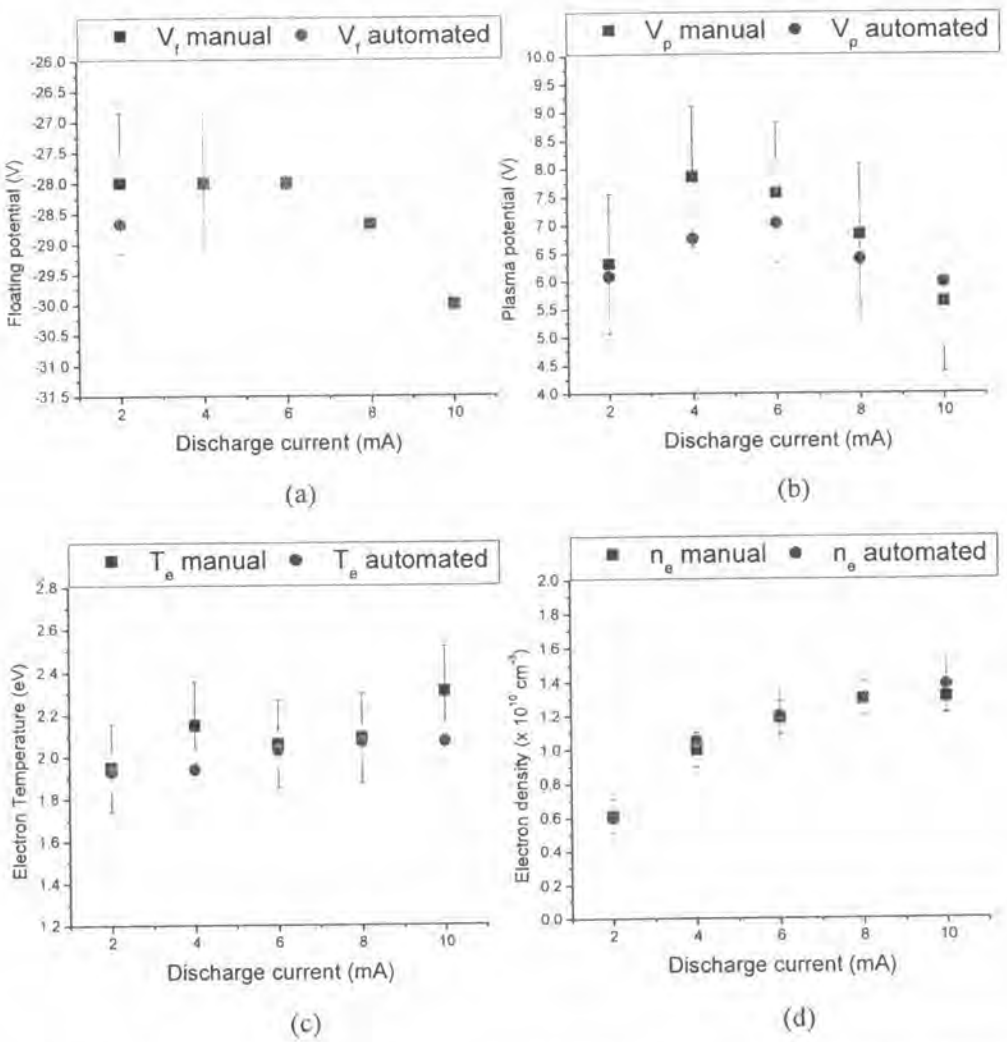

Figure 5.3: The comparative results at pressure 0.6 torr between the manual calculation and the automated algorithm in analyzing (a) floating potential, (b) plasma potential, (c) electron temperature, and (d) electron density.

In conclusion, the automated algorithm shows a good agreement with the manual calculation in analyzing four plasma parameters. The average values of floating potentials at pressures 0.6 – 1.0 torr are between -28.53 V and -37.24 V with ± 1.15 V for both the manual calculation and the automated algorithm. For plasma potential at pressures 0.6 – 1.0 torr, the automated algorithm yields 5.62 ± 1.51 V,

while the manual calculation yields 6.40 ± 1.24 V. For electron temperature in this pressure range, the automated algorithm yields the temperature around 2.05 ± 0.09 eV which agrees with the manual calculation (2.14 ± 0.21 eV). At pressure 0.6 torr, electron densities of both the automated algorithm and the manual calculation are around (1.11 ± 0.16) x 10^{10} cm^{-3} (1.08 ± 0.10) x 10^{10} cm^{-3}, respectively. And electron densities at pressures between 0.8 and 1.0 torr are around (5.60 ± 0.16) x 10^{10} cm^{-3} for the automated algorithm and around (5.73 ± 0.10) x 10^{10} cm^{-3} for the manual calculation.

5.2 Analytical Results of AC Discharge

In the electrical probe measurement in the AC (50 Hz) discharge system, Argon plasma was also carried out. The probe was placed at the center of the electrodes which were supplied with AC (50 Hz) signal of 1,000 V. The measurements were performed at diverse pressures from 0.3 to 1.0 torr. An example of the probe measurement at pressure 0.3 torr is depicted in figure 5.4. The I-V characteristic obtained from the AC discharge differs from the characteristic of the DC discharge.

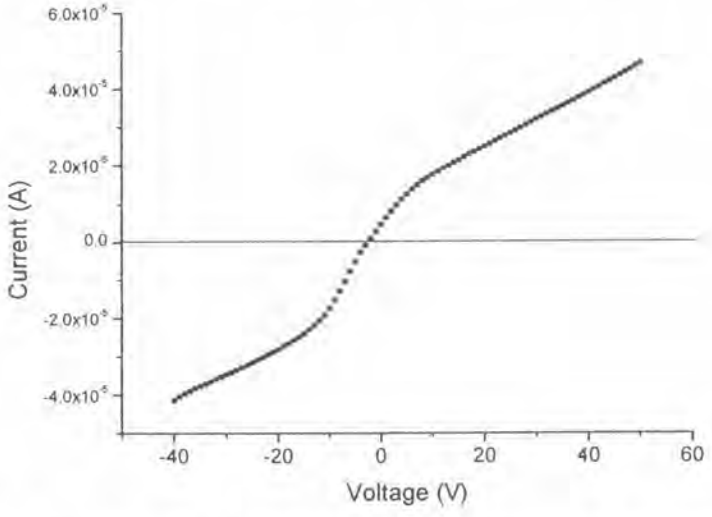

Figure 5.4: An example of an AC discharge probing measurement at pressure 0.3 torr shows the current is vertically symmetric at zero current.

From the example of the I-V data at pressure 0.3 torr in figure 5.4, the current is vertically symmetric at zero current. In this case, the curve shows similarity to the

double-probe measurement with two exploring-probe tips supplied with a voltage source with respect to each other [15,27,28]. With the double-probe measurement, the I-V characteristic will have a half in the positive current and the other half in the negative one. From the AC discharge probing measurement, this might be because of the conventional frequency (50 Hz) of the AC source in use. At low frequency, the potentials of the two electrodes are alternated in time variance. This makes the plasma alternating as well. Then, the probe current that comes from charged particles flowing through the probe appears the characteristic like the double-probe measurement.

Figures 5.5(a) – 5.5(e) show the analytical results of plasma parameters between the manual calculation and the automated algorithm obtained from I-V characteristics in the AC discharge. From the comparative results between the manual calculation and the automated algorithm, the automated algorithm yields floating and plasma potentials near to those potentials of the manual calculation in figure 5.5(a) and 5.5(b). This is because floating potential directly determines from I-V characteristic when current approaches to zero. For plasma potential, the automated algorithm can divide the I-V curve of the AC discharge into three intervals in order to determine plasma potential. However, for electron temperature, the comparative results between the automated algorithm and the manual calculation are quite different as shown in figure 5.5(c). The automated algorithm yields electron temperature around 3.85 ± 0.24 eV at pressure 0.3 – 1.0 torr, but the temperature of the manual calculation is around 2.99 ± 0.40 eV at the same pressure range. The difference of the temperature between the manual and automated analyses comes from the I-V curve of the AC discharge because the process in interpretation of the single probe characteristic cannot apply to the double probe curve. It is evident when the manual calculation and the automated algorithm are used to analyze plasma density, electron density (figure 5.5(d)) and ion density (figure 5.5(e)). From the assumption of quasi-neutrality ($n_e \approx n_i$), the analytical results do not correspond with the assumption because both the manual calculation and the automated algorithm yield electron density in order 10^7 cm^{-3}, but ion density up to order 10^9 cm^{-3}. Therefore, both the manual calculation and the automated algorithm cannot apply to analyze plasma parameters accurately, if I-V data is similar to double probe characteristic.

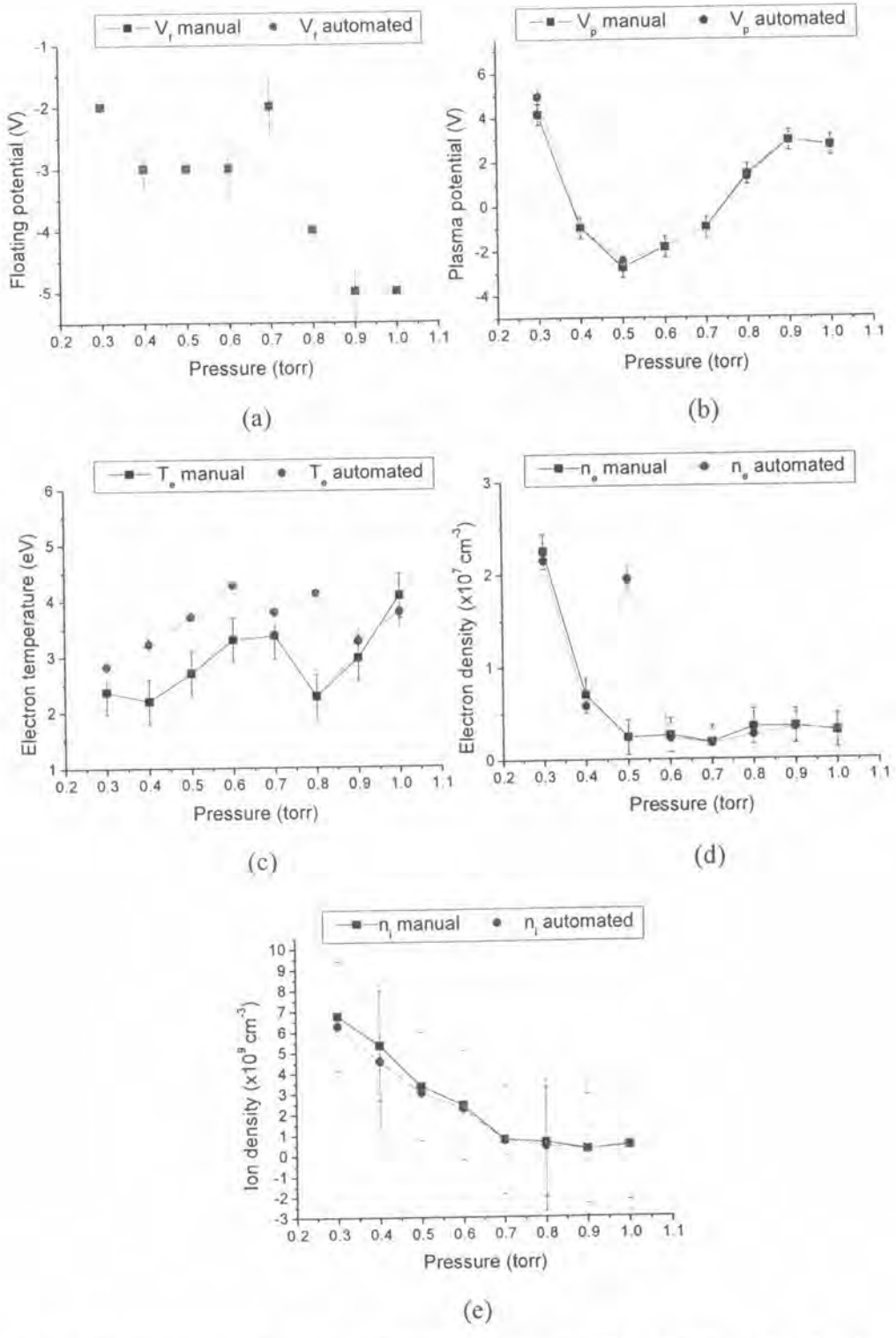

Figure 5.5: The analytical results of plasma parameters, (a) floating potential, (b) plasma potential, (c) electron temperature, (d) electron density, and (e) ion density between the manual calculation and the automated algorithm.

5.3 Analytical Results of RF Discharge

For the experimental data measured in the RF discharge system by the compensated electrical probe, Argon plasma was also carried out in similar fashion. Set of measurements are done by varying pressures from 0.5 to 1.1 torr and powers dissipated into the plasma between 10 and 50 W. Figure 5.6 illustrates an example of the I-V curve acquired from the probe measurement.

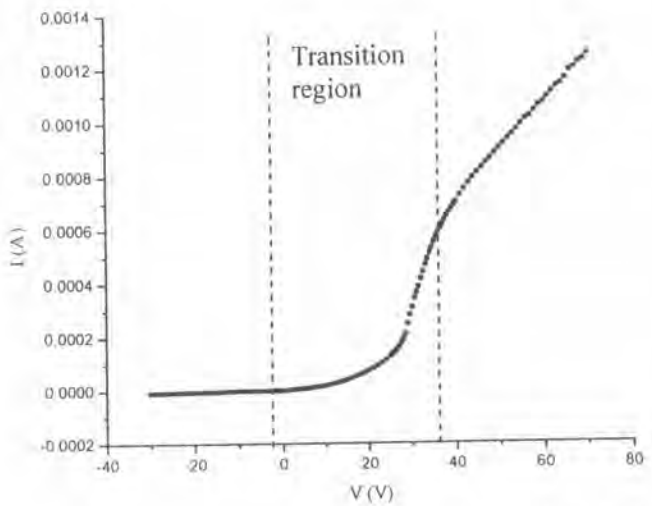

Figure 5.6: An example of I-V curve obtained from the RF discharge.

From figure 5.6, it can be seen that the I-V curve in the transition region tends to have two electron temperature, low and high temperatures. By taking current with natural log, one can see that there will be two changes in the transition region of the graph of natural log current and voltage as shown in figure 5.7. The change of natural log current in the low temperature range will rapidly increase, which corresponds to current transiting the ion-saturation into the transition region. After the low temperature range, the natural log current will gradually increase which yield high electron temperature.

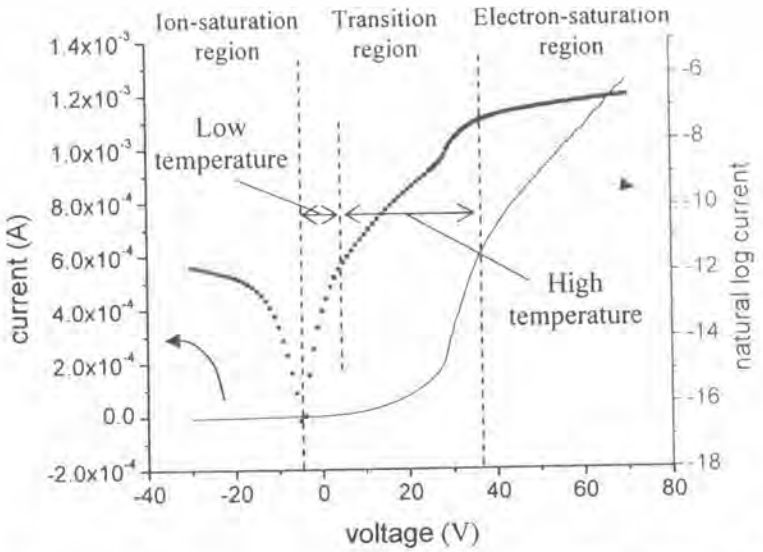

Figure 5.7: The current-voltage curve (solid line) in correspondence with natural log current curve (dot line) with two electron temperatures, low and high temperatures.

The analytical results of electron temperature are shown in figures 5.8(a) – 5.8(e). The manual calculation can analyze both low and high electron temperatures, while the automated algorithm can only find high temperature one. From the result, low electron temperatures obtained from the manual calculation are around 2 – 4 eV with ± 0.79 eV for all pressures and powers. These temperatures gradually decrease with increasing pressures, which correspond to many researches [15,18,21,23,26]. This is because, at a high pressure, there are much particles increasing, in which electrons undergo many collisions and lose their energy in these collisions. However, in RF probing measurement, we further found that I-V characteristics also have high electron temperature around 6 – 8 eV with ± 0.94 eV in the manual calculation. This temperature may come from many sources, such as RF interference, secondary electrons, or effective collecting area of probe, that have an effect on I-V data. For finding two electron temperatures, it generally occurs in the probing measurement which corresponds to other research articles [6,8,18].

For the analytical result of the automated algorithm, the algorithm can only estimate high electron temperature and yield the temperatures around 6 – 7 eV with ± 0.86 eV, as shown in figure 5.8(a) – 5.8(e). In comparing with high temperature obtained from the manual calculation, the automated algorithm under-estimated the

temperature. This results from the process in defining the ion-saturation region between the manual calculation and the automated algorithm.

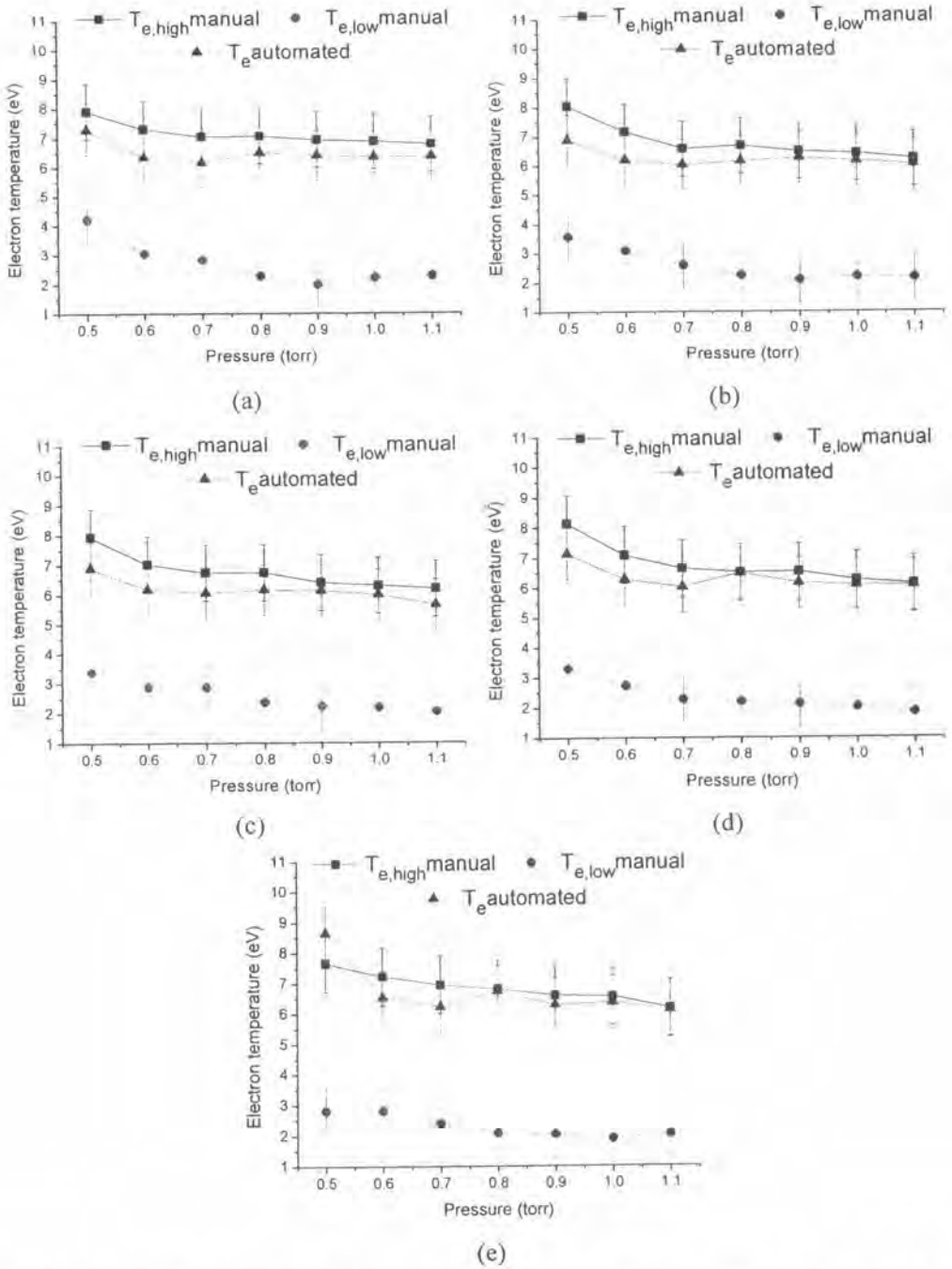

Figure 5.8: The analytical results of electron temperature between the manual calculation and the automated algorithm at the dissipated powers of (a) 10 W, (b) 20 W, (c) 30 W, (d) 40 W, and (e) 50 W.

There are two causes that affect on the estimation of electron temperature. The first cause directly depends on the range in the temperature calculation. As seen in the result of the RF discharge, electron temperature has two electron temperatures. These temperatures depend on the range in the graph of ln I_e vs V, as appeared in figure 5.7. The other cause which indirectly affect on the estimation of electron temperature is to define ion-saturation region or ion current. The ion-saturation region which is usually used to define ion current can decrease electron temperature as illustrated in figure 5.9. The automated algorithm will take current of the transition region into account as the ion-saturation region. In this case, the algorithm will lose data of low electron temperature, and ion current (in figure 5.9) will be more slope than ion current obtained from the manual calculation. The higher slope of ion current will cause a change in electron current (I_e), which is the remaining current after subtracting ion current out from I-V curve. This change will have an effect on electron temperature under-estimation, as appeared in figure 5.8(a) – 5.8(e) of the automated algorithm analysis. Using inaccurate ion-saturation region of the automated algorithm, not only give an effect on electron temperature, but also affects on the estimation of ion density.

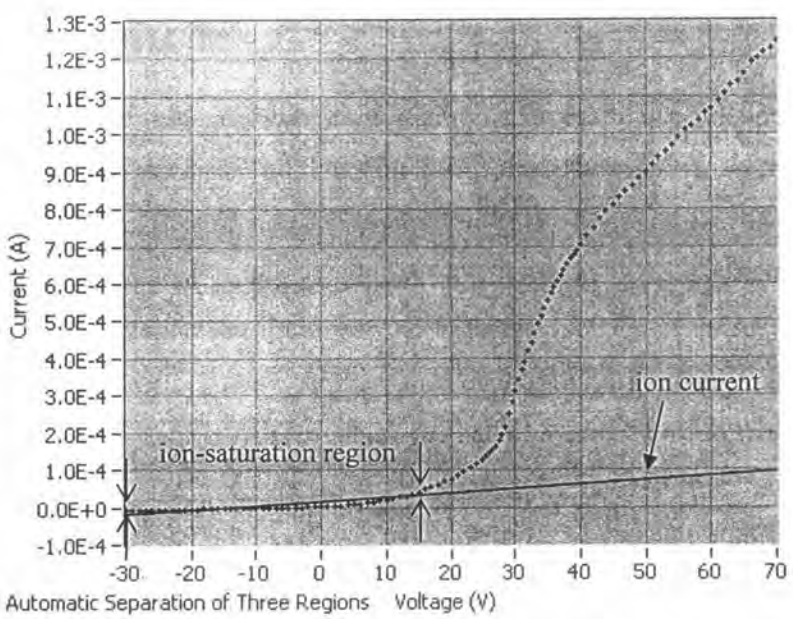

Figure 5.9: The effect of defining ion-saturation region and extrapolating ion current on the under-estimation of electron temperature in the automated algorithm.

Figure 5.10(a) – 5.10(e) show the analytical results of ion density at various plasma igniting conditions. From the result, the automated algorithm yields ion density higher than the density obtained from the manual calculation. This is because of different defining of the ion-saturation region in the automated algorithm, which yields the deviated intercept of ion current as illustrated in figure 5.11. From figure 5.11, the automated algorithm defines ion-saturation current ($I_{i,sat}$) higher than the manual calculation. Therefore, the higher $I_{i,sat}$ will increase the estimation of ion density in equation (2.18).

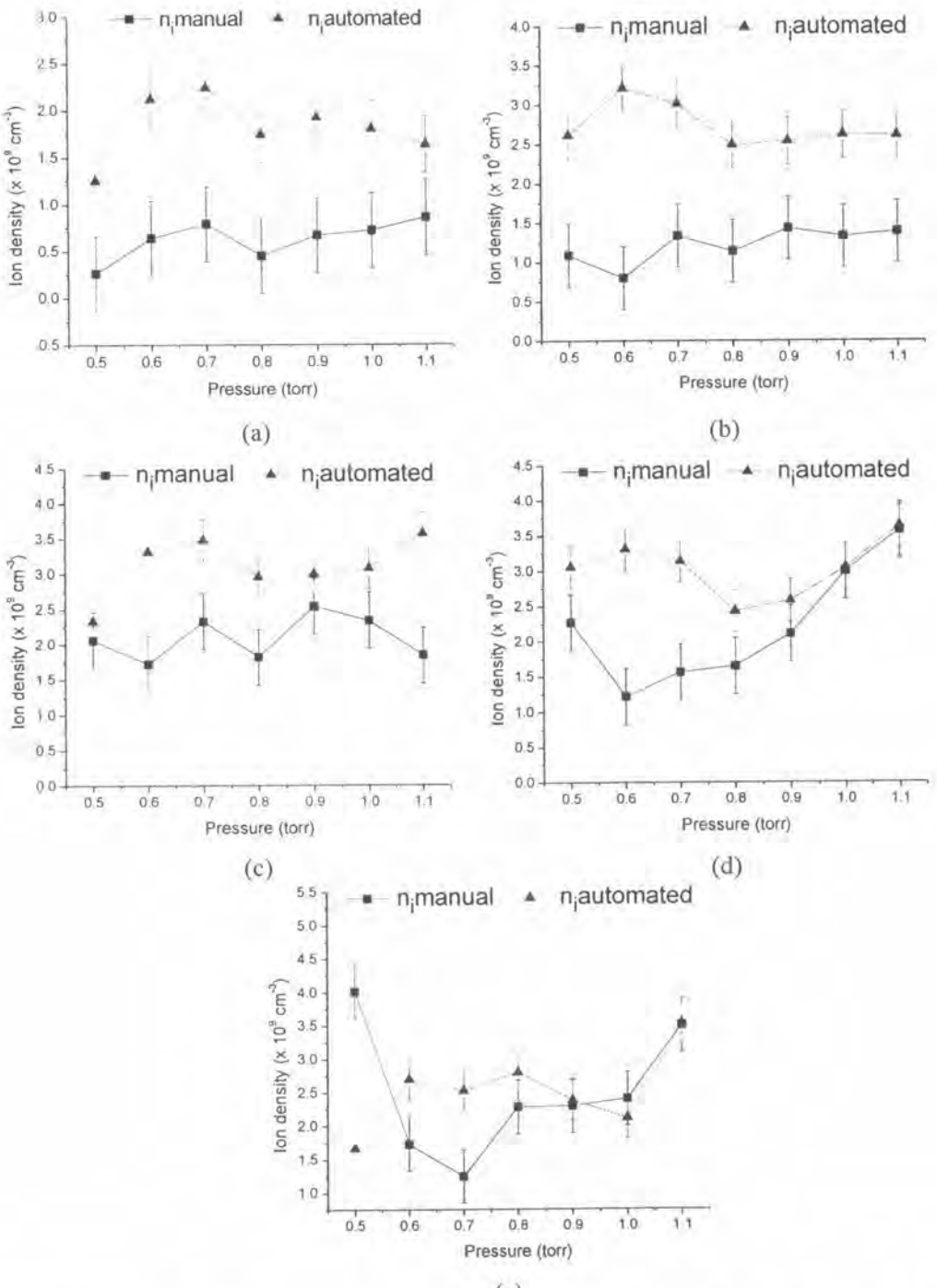

Figure 5.10: The analytical results of ion density between the manual calculation and the automated algorithm at the dissipated powers of (a) 10 W, (b) 20 W, (c) 30 W, (d) 40 W, and (e) 50 W.

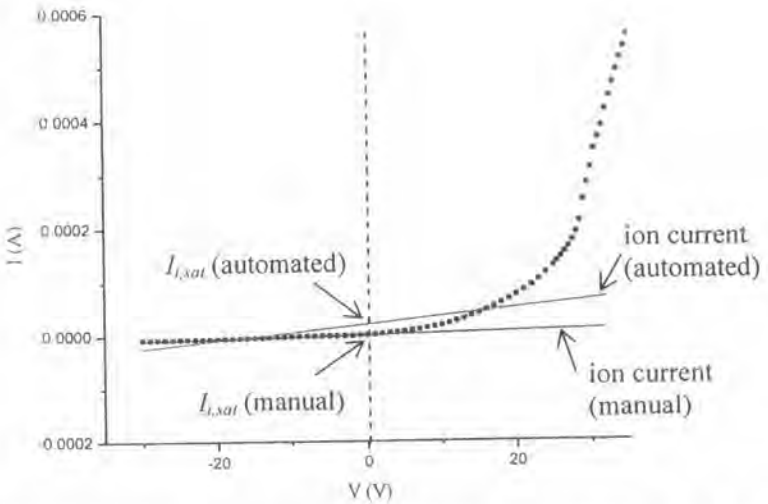

Figure 5.11: Dependence of ion-saturation current ($I_{i,sat}$) on the intercepts of ion current between the automated algorithm and the manual calculation that affect on ion density.

For the other parameters, figure 5.12(a) – 5.12(c) show the analytical results of floating potential, plasma potential, and electron density at dissipation power 20 W between the manual calculation and the automated algorithm. The automated algorithm yields floating potential (figure 5.12(a)) that well agrees with the manual calculation. The floating potential results tend to decrease from -2 ± 1.07 V at pressure of 0.5 torr to -7 ± 1.07 V at pressure of 1.1 torr. For plasma potential in figure 5.12(b), the result of the automated algorithm corresponds to the result analyzed by the manual calculation. The tendency of plasma potential decreases with the increase of pressure, which can be directly observed from figure 5.13. The interception of two straight lines in the transition and electron-saturation regions shifts toward lower voltage with increasing pressure (the tendency line in figure 5.13). Not only does the plasma potential decrease, but the electron-saturation current ($I_{e,sat}$) also decreases with the increasing pressure. Therefore, the decrease of $I_{e,sat}$ will lessen the electron density when pressure increases, as shown in figure 5.12(c).

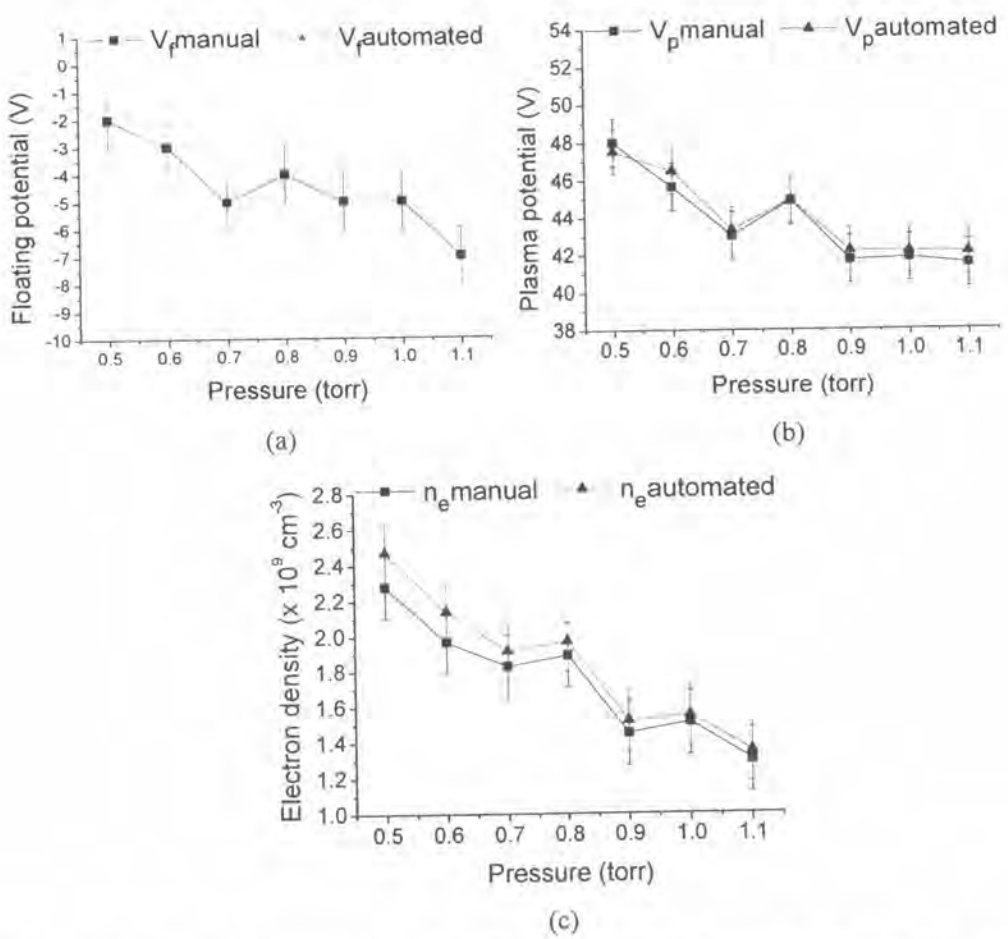

Figure 5.12: The analytical results of (a) floating potential, (b) plasma potential, and (c) electron density at dissipated power 20 W between the manual calculation and the automated algorithm.

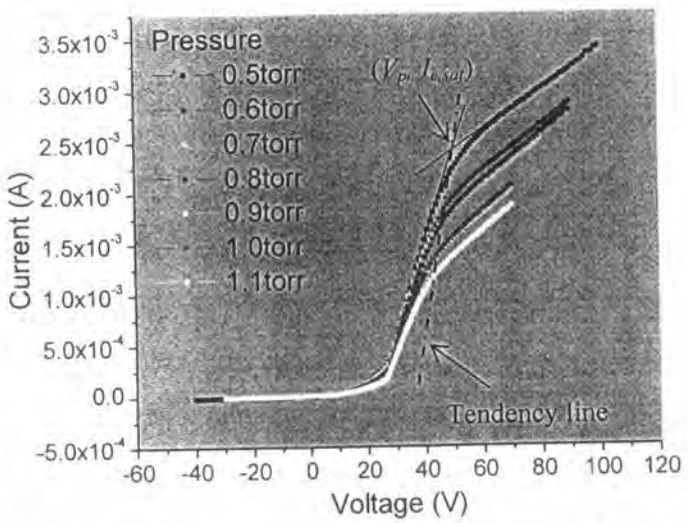

Figure 5.13: The tendency of plasma potential and electron-saturation current ($I_{e,sat}$) in I-V characteristic decreasing with the increase of pressure.

5.4 Advantages of the Automated Algorithm

Most I-V data analyses to obtain plasma parameters are generally carried out by manual calculation with computer assistance. In manual calculation process, I-V data need to be stored and then analyzed plasma parameters. This process will consume time and require highly qualified personnel in interpretation of I-V data in real-time. In this work, the automated algorithm can analyze plasma parameters from I-V data. The algorithm will also reduce time consuming and automatically analyze such parameters.

In the interpretation of I-V characteristics, the characteristic can be divided into three regions, ion-saturation, transition, and electron-saturation regions. By differentiating I-V characteristic, two linear responses beside the maximum of the first derivative will appear in correspondence with ion and electron saturation regions. And if we further differentiate the first derivative, the interval from maximum to minimum of the second derivative will correspond to transition region. Therefore, we utilize these characteristics in developing the automated algorithm to analyze plasma parameters.

From the analytical result, the automated algorithm can analyze plasma parameters that are well agrees with the result of the manual calculation. Floating potential, which is typically defined from current approaching to zero, is in a good agreement between the automated algorithm and the manual calculation. The automated algorithm yields floating potential equal to the manual calculation at all plasma discharges.

In determining plasma potential and electron-saturation current, these values directly depend on how we define the transition and electron-saturation regions. The intercept of linear fitting in these ranges is used to define plasma potential and electron-saturation current. The automated algorithm can separate these regions by using linear response of the first derivative for electron-saturation region, and the interval from maximum to minimum of the second derivative for transition region. By utilizing these characteristics, the automated algorithm can yield plasma potential and electron-saturation current (as appeared in electron density) in correspondence with those of the manual calculation.

For ion current and ion-saturation current, the automated algorithm utilizes linear response of the first derivative to define ion-saturation region. This region will be used to generate ion current. And the intercept of ion current is then used as ion-saturation current to estimate ion density.

In calculation of electron temperature, the interval between maximum of the first derivative and end position of ion-saturation region will be used for the automated algorithm. In the graph of $\ln I_e - V$, this interval will yield electron temperature close to the temperature of the manual calculation.

However, in estimating plasma parameters, the automated algorithm has some limitations that may yield such parameters different from the manual calculation. These limitations include measured I-V data and two electron temperatures that affect on the estimated result of the automated algorithm.

5.5 Limitations of the Automated Algorithm

Although the automated algorithm developed from the manual calculation, there are limitations of the algorithm which will yield error in analyzing plasma parameters. This error may result from I-V probing measurement of plasma with two electron temperatures. In some experimental data, I-V characteristics have some current points overshooting or discrete in some ranges, as seen in figure 5.14. The overshooting current in figure 5.14 will cause error in defining ion current which leads to error in estimation of ion density and electron temperature as discussed in section 5.3. The discrete current will cause error in estimating plasma potential as seen in the analytical result of DC discharge. Including I-V data obtained from the AC discharge, the automated algorithm cannot analyze I-V characteristic which is similar to the characteristic of double probe. Another I-V characteristic that the automated algorithm cannot analyze plasma parameters is fluctuating current.

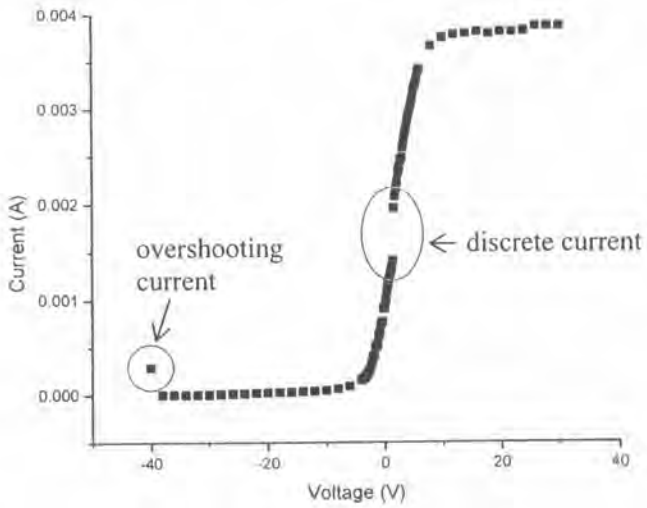

Figure 5.14: Overshooting and discrete current in I-V characteristic that causes error in analyzing plasma parameters of the automated algorithm.

Figure 5.15 shows fluctuating current in probe measurement. When current transits the transition region to the electron-saturation region, current will become fluctuating. The fluctuating current in some measurements will affect on the first and second derivatives. The maximum and minimum positions of the first and second

derivatives will take place in the electron-saturation region, instead of the transition region. The wrong positions yield that the automated algorithm cannot separate I-V curve into three regions nor analyze plasma parameters. Furthermore, overlap of current in I-V data also causes the automated algorithm unable to analyze such parameters, as illustrated in figure 5.16. This is because the algorithm cannot calculate the first and second derivatives from figure 5.16.

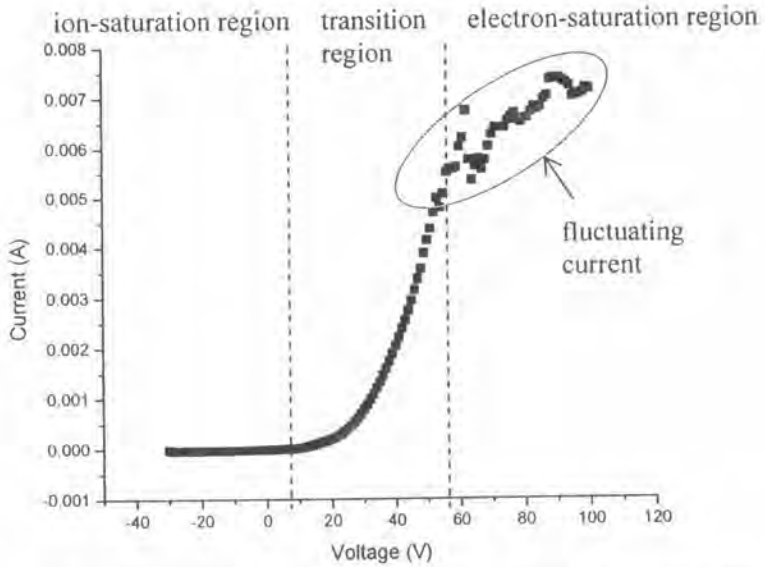

Figure 5.15: Fluctuating current in electron-saturation region that causes the automated algorithm cannot analyze plasma parameters.

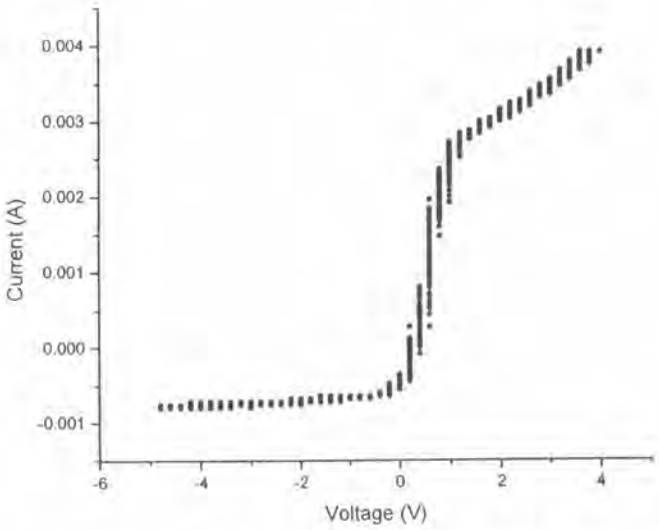

Figure 5.16: Overlap current in I-V characteristic that causes the automated algorithm cannot analyze plasma parameters.

Another limitation of the automated algorithm is that of plasma with electron of two temperatures. In this case, the algorithm cannot separate two electron temperatures, as discussed in the result of RF discharge. Therefore, the automated algorithm is best used to estimate plasma with single electron temperature.